Metal nanoparticle arrays for near field optical lithography

Pieter G. Kik,[*] Andrea L. Martin, Stefan A. Maier, and Harry A. Atwater
Thomas J. Watson Laboratory of Applied Physics, California Institute of Technology,
Pasadena, CA 91125, USA

ABSTRACT

We have recently proposed a new approach to optical lithography that could be used to replicate arrays of metal nanoparticles using broad beam illumination with visible light and standard photoresist. The method relies on resonant excitation of the surface plasmon oscillation in the nanoparticles. When excited at the surface plasmon frequency, a resonantly enhanced dipole field builds up around the nanoparticles. This dipole field is used to locally expose a thin layer of photoresist, generating a replica of the original pattern in the resist. Silver nanoparticles on photoresist can be resonantly excited at wavelengths ranging from 410 nm to 460 nm, allowing for resonantly enhanced exposure of standard g-line photoresist. Finite Difference Time Domain (FDTD) simulations of isolated silver particles on a thin resist layer show that broad beam illumination with p-polarized light at a wavelength of 439 nm can produce features as small as 30 nm, or $\lambda/14$. Depending on exposure time lateral spot sizes ranging from 30 to 80 nm with exposure depths ranging from 12 to 45 nm can be achieved. We discuss the effect of particle-particle interactions in the replica formation process. Experiments on low areal density Ag nanoparticle arrays are discussed. Resist layers (thickness 75 nm) in contact with 40 nm Ag nanoparticles were exposed using 410 nm light and were subsequently developed. Atomic Force Microscopy on these samples reveals nanoscale depressions in the resist, providing evidence for plasmon-enhanced resist exposure.

Keywords: lithography, contact printing, surface plasmon, nanoparticles, pattern replication, plasmon waveguides

1. INTRODUCTION

The continuing size reduction of integrated circuits to nanometer scale dimensions requires the development of new lithographic techniques. It is becoming increasingly complex and costly to use the established method of optical projection lithography at the short optical wavelengths required to reach the desired feature sizes. For example, the use of wavelengths in the deep ultraviolet,[1] the extreme ultraviolet (EUV),[2] or the X-ray regime[3] requires radical changes in the lithographic process, including the development of new light sources, photoresists and optics. This is seen as a major problem in the industry, as evidenced by large scale efforts to develop alternative approaches to nanolithography.

A relatively established method for the production of high-resolution patterns is the use of focused particle beams, e.g. a focused electron beams[4] or ion beams,[5] that expose a resist layer as it is scanned across the substrate. Although this produces high-resolution patterns, the sequential nature of the technique results in long writing times. Other sequential techniques involve the use of a local probe such as the tip of an Atomic Force Microscope (AFM)[6] or the tip of a Near-field Scanning Optical Microscope (NSOM).[7] Two parallel approaches to nanolithography that do not require short-wavelength light are micro-contact printing,[8] evanescent near field lithography (ENFOL)[9] and evanescent interferometric lithography (EIL).[10] The latter two methods employ the evanescent optical field set up directly below a contact mask for exposure, and promise a resolution as high as $\lambda/20$.[11] We have recently proposed[12] a new approach to nanolithography which we have called 'plasmon printing'. The method relies on the surface plasmon resonance occurring in metal nanoparticles, and can produce sub-wavelength structures using broad beam illumination of standard photoresist with visible light.

---

[*] E-mail: kik@caltech.edu

2. THEORY

Plasmon printing relies on the plasmon resonance occurring in nanoscale metallic structures. When a metallic nanoparticle is placed in an optical field, it can exhibit collective electron oscillations known as surface plasmon oscillations. If the diameter of the particle is much smaller than the applied wavelength, the oscillating charges produce an oscillating dipole field around the particle. When the excitation occurs resonantly, i.e. when the excitation frequency coincides with the natural relaxation frequency of the particle, this can result a strongly enhanced electrical field near the particle. If the resonance frequency falls within the sensitivity range of a photoresist, this field enhancement can be used to locally expose a thin layer of resist.

A schematic of the printing process is shown in Fig. 1. A transparent mask containing metal particles near its surface is brought into intimate contact with a thin layer of photoresist. The resist covered substrate is then illuminated with p-polarized light at the plasmon resonance frequency of the particles. The resulting enhanced optical field around the metal particles will cause increased exposure of the resist layer directly below the particles. The exposure is interrupted when the exposure threshold is reached in the resist directly beneath the particles. Although the whole resist film has been illuminated, subsequent development of the resist will only affect the areas that received locally enhanced exposure. In this way a replica of the mask pattern is produced in the resist layer.

The choice of particle material depends on the required wavelength – the resonance wavelength should fall within the resist sensitivity. In order to be able to use standard g-line photoresist, the resonance wavelength should lie between 300 nm and 460 nm. Additionally, to obtain high field enhancement, long electron scattering times are desirable. Silver is a good candidate, with long reported electron scattering times[13] up to 10 fs and a resonance occurring at a wavelength of ~360 nm in air. The resonance frequency is not a fixed quantity: for a spherical particle, the surface plasmon resonance occurs at the wavelength λ for which $\varepsilon_{particle}(\lambda) = -2\varepsilon_{matrix}(\lambda)$ with $\varepsilon_{particle}$ and ε_{matrix} the real part of the dielectric functions of the particle and the surrounding material respectively. Consequently, the wavelength at which resonance occurs can be tuned by changing the refractive index of the surrounding material. The dielectric function of metals is negative around the resonance frequency and increases in magnitude as the wavelength is increased. This means that the plasmon resonance will shift to longer wavelengths as the refractive index of the surrounding material is increased. Eventually, for sufficiently high refractive index (n_{matrix}=1.8) the resonance wavelength may be shifted outside the sensitive region of g-line photoresist. This puts constraints on the nanoparticle surroundings, and thus on the mask materials that can be used.

For high field enhancement, the phase of the optical field should be approximately constant over the particle volume. When large particles are used, the field enhancement will drop due to the excitation of multipolar oscillations in the particles. In practice this means that the particles should have a diameter on the order of 0.1λ or smaller, with λ the illumination wavelength. For particles in this size range, electron relaxation due to surface scattering becomes significant. This surface scattering becomes more important for smaller particle diameters, and adversely affects the field enhancement. In this article, we therefore focus on particles with a diameter of ~0.1 λ.

A final consideration is the incidence angle. Since the particle polarization is induced by the electric field of the incoming wave, p-polarized light propagating approximately parallel to the resist layer will produce a maximum field enhancement directly above and below the particle, giving high exposure contrast. As we will show below, exposing at an angle approximately 70° off the surface normal improves the obtained feature size compared to perfect glancing incidence illumination.
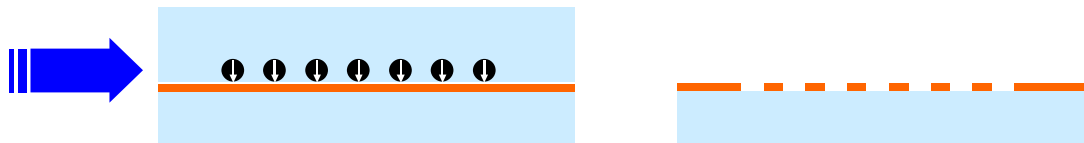

Figure 1 Schematic representation of plasmon printing, showing (a) glancing angle illumination using polarized visible light, producing enhanced resist exposure directly below the metal nanostructures in the mask layer, and (b) the resulting pattern in the resist layer after development.

3. SIMULATIONS

The details of the plasmon printing process depend on the magnitude of the field enhancement effect and the exact spatial field distribution around the metal nanoparticles. Field distributions during illumination were calculated using 3D Finite Difference Time Domain (FDTD) calculations. The simulated geometry consists of a 40 nm diameter silver particle on a 50 nm thick resist layer (modeled as a purely dielectric layer with a refractive index n=1.7) on glass (n=1.4). The silver particle is embedded in an index matched medium (n=1.4), which could for example be a conformable PDMS mask. The simulation volume contains ~4×10^6 mesh points with a graded mesh density to obtain a high mesh density around the silver particle (mesh spacing 2 nm) while keeping the total number of mesh lines manageable. The particle is excited by a p-polarized plane wave coming in at glancing angle (between 70° to 90° off the surface normal). The complex dielectric function $\varepsilon(\omega)$ of silver is approximated by a Drude model, given by

$$\varepsilon(\omega)=1-\frac{\omega_p^2}{\omega^2-i\omega\gamma}$$

with ω the angular frequency of the optical field, ω_p the bulk plasma angular frequency, and γ the electron collision frequency defined as $\gamma=1/\tau$ with τ the average time between subsequent electron collisions. The electron collision frequency is set to 10^{14} s^{-1} taken from Ref. 13, corresponding to τ=10 fs. The value for ω_p is set to 1.08×10^{16} rad/s in order to have the Drude dielectric function coincide with literature values for $\varepsilon(\omega)$ around λ=430 nm. The total length of the simulation is 30 fs or ~20 optical cycles, ensuring that the amplitude of the field oscillation in and around the particle has reached its steady state. The time step used in the simulations is two attoseconds or 1/750 of an optical cycle.

      Figure 2(a) shows a snapshot of the calculated field energy density around the 40 nm silver particle under plane wave excitation at 439 nm. The optical wave is traveling in the +x direction (incidence angle of 90° relative to the surface normal). High color intensity in the plot corresponds to high local energy density. The vertical arrows indicate
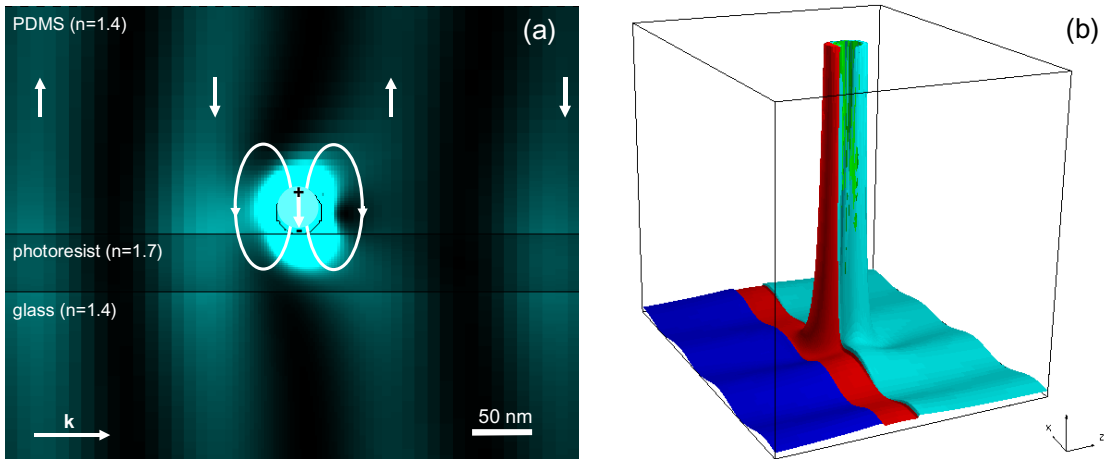

Figure 2 (a) Snapshot of the local field energy density distribution around a 40 nm silver particle on photoresist under illumination with p-polarized light (λ=439 nm) at the surface plasmon resonance frequency, as obtained from 3D Finite Difference Time Domain simulations. The vertical arrows indicate the direction of the electric field in the illuminating wave. (b) Idem, with intensity plotted on the vertical axis to emphasize the spatial dependence of the energy density. A strongly enhanced (instantaneous) intensity is observed directly beneath the particle.
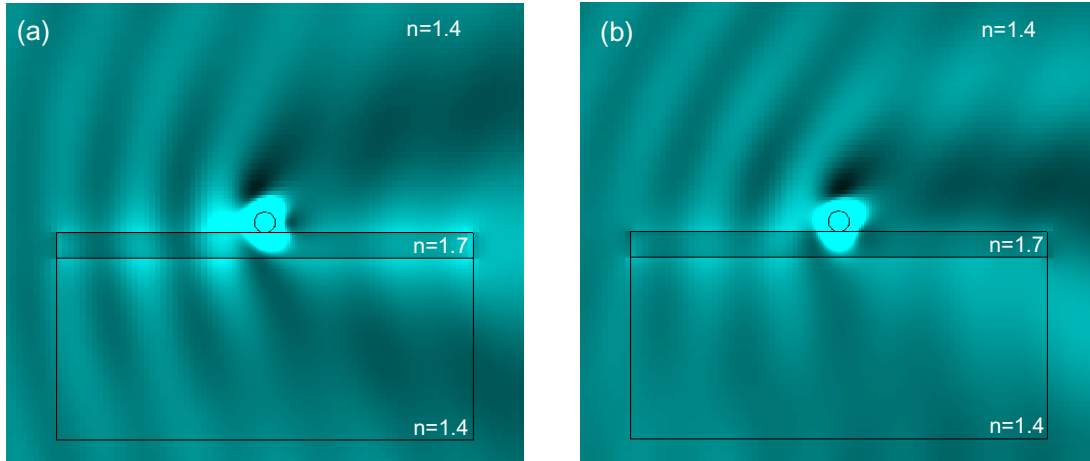
Figure 3   Time averaged intensity plots around 40 nm silver particles on photoresist under illumination with p-polarized light (λ=439 nm) at the surface plasmon resonance frequency, as obtained from 3D Finite Difference Time Domain simulations, for illumination angles of (a) 90° compared to the surface normal and (b) 70° compared to the surface normal. Illumination under a finite angle is seen to produces a well area of enhanced exposure.

the direction of the electric field. The image shows the situation in which a positive wavefront (field up) has just passed the particle. This wavefront has induced a strong opposing field inside the particle with a corresponding dipole field around the particle, as indicated schematically by the curved field lines. The particle has a π/2 phase lag compared to the exciting wave, which is a signature of resonant excitation. Note the enhanced energy density around the particle compared to the exciting wave. Figure 2(b) shows a hill plot of the energy density.

The field snapshot in Fig. 2 gives a first indication of the spatial extent of the enhanced field, but it is the time averaged intensity that determines the exposure. Figure 3(a) shows the energy density around the silver nanoparticle excited under the same conditions as in Fig. 2 averaged over a full optical cycle. Several things can be noted: Firstly, directly below the particle an area of enhanced exposure is visible, extending ~40 nm into the resist layer, with a width of ~80 nm. The intensity beneath the particle drops rapidly with distance, and consequently the exposed spot size can be tuned by varying the intensity and exposure time. Secondly, the intensity distribution around the particle is asymmetric, showing an extended high intensity region to the left of the particle. This asymmetry is caused by the phase lag between illuminating wave and particle response. The dipole field near the nanoparticle is π/2 out of phase with the exciting wave. As can be seen in Fig. 2(a) this dipole field interferes destructively with the wavefront to the right of the particle, and constructively with the approaching wavefront to the left of the particle. Interference of the induced dipole radiation with the incoming wave also the causes the standing wave pattern observed in the left part of Fig. 3(a), and the dark bands in the top right and bottom right of the figure. The asymmetry in the exposed area observed in Fig. 3(a) can be reduced by changing the angle of incidence of the incoming light. Figure 3(b) shows the time averaged field density around the particle as obtained at an illumination angle of 70° off the surface normal. The region of enhanced intensity to the left of the particle now occurs mostly above resist layer, while the region of enhanced exposure in the resist layer is more symmetrical.

Figure 4(a) shows the logarithm of the averaged energy density for the case of illumination at 70° in a contour plot. The contour lines are iso-intensity lines separated by 1 dB (~26% intensity change) and the full scale spans a factor 10^4. The high intensity features near the Ag nanoparticle are artifacts resulting from the sharp edges on the meshed sphere surface. The iso-intensity lines indicate what kind of resolution can be obtained with plasmon printing. In the case of a real exposure, the resist surface remaining after the development stage will follow the iso-intensity line at which the exposure threshold of the resist was reached. A long exposure time will thus produce a deep and relatively wide depression in the resist. Figure 4(b) shows how the width of the exposed spot (measured ~10 nm beneath the surface) depends on the exposure depth. From this plot it can be seen that a lateral feature size of 0.1λ can be achieved with an exposure depth of 17 nm.
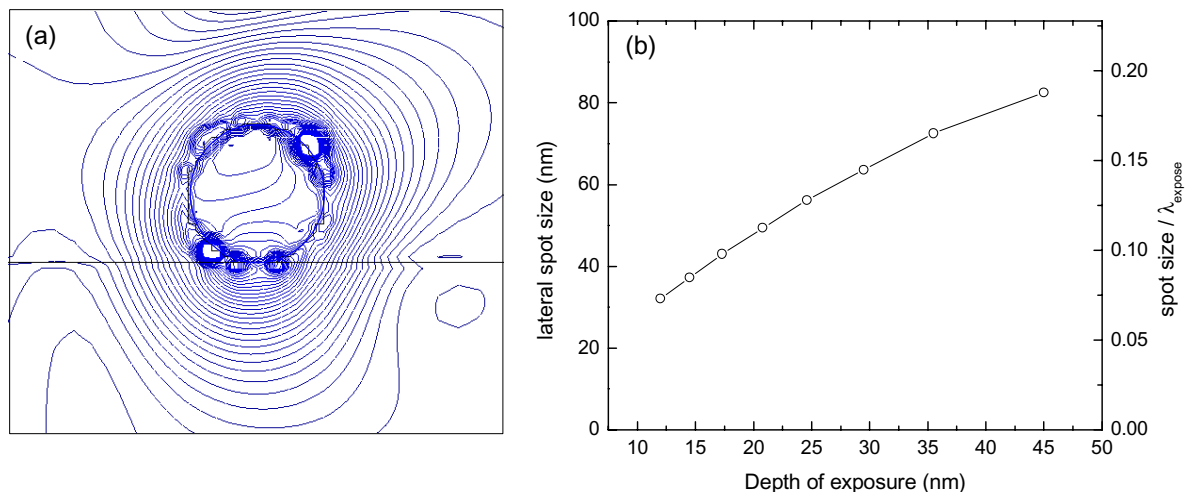
Figure 4 (a) Contour plot of the time averaged intensity around a 40 nm silver particle on a 50 nm thick photoresist layer under illumination with p-polarized light (λ=439 nm) at the surface plasmon resonance frequency, as obtained from 3D Finite Difference Time Domain simulations at an illumination angles of 70° compared to the surface normal. (b) Plot of the relation between the lateral feature size and exposure depth as the exposure time is varied.

All calculations shown above dealt with isolated silver particles. When using dense arrays of metal particles, nearest-neighbor interactions can influence the resonance frequency. We have observed experimentally that the resonance wavelength of linear arrays of 50 nm gold particles with a center-to-center spacing of 75 nm on indium-tin-oxide can shift by as much as 19 nm depending on the polarization of the incoming light.[14] For a polarization along the particle array under normal incidence illumination the resonance shifts to 604 nm compared to 590 nm for isolated particles. For polarization normal to the particle array the resonance shifts to 585 nm. The latter situation most closely resembles the situation of glancing angle illumination desired in plasmon printing. The presence of different closely spaced nanoparticle arrays within a single mask could in principle result in uneven exposure, since some structures may
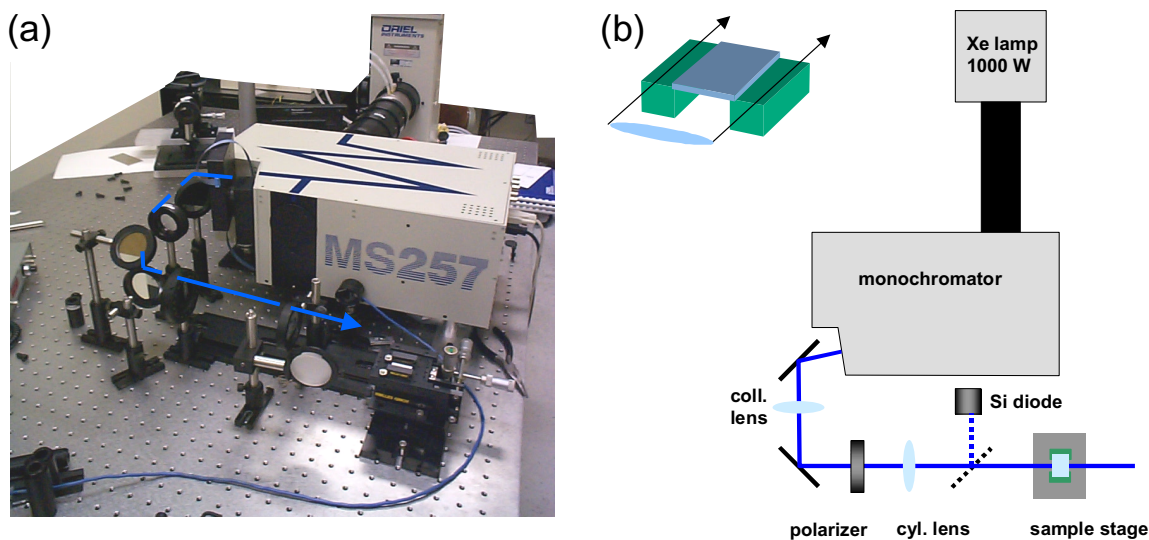

Figure 5 (a) Photograph and (b) schematic representation of the illumination setup. A enlarged schematic of the sample holder is included, showing the approximate beam size. The beam direction is indicated by the arrows.
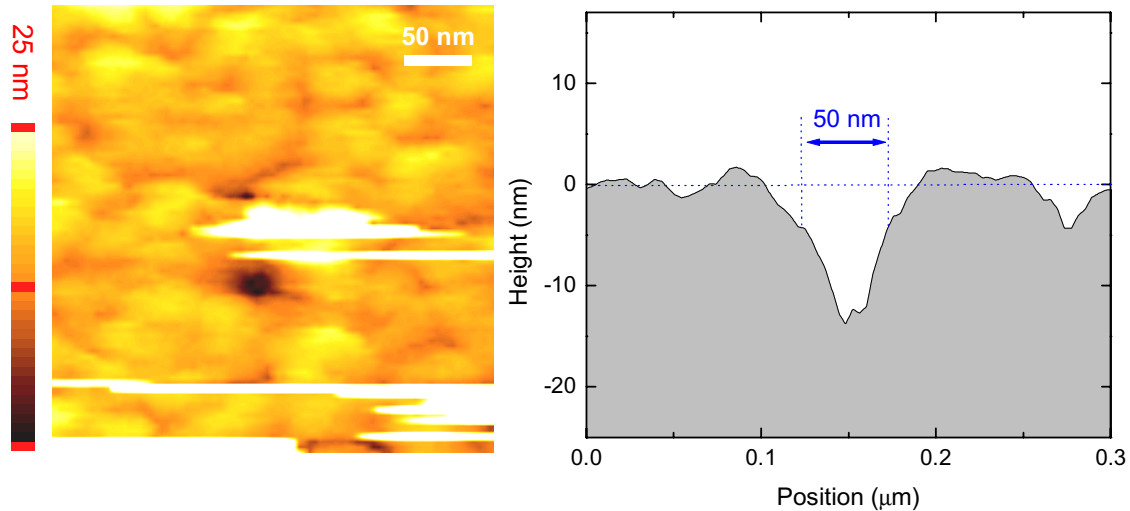
Figure 6 (a) Atomic Force Microscopy image of a 75 nm thick exposed and developed AZ1813 resist layer, showing the presence 41 nm Ag particles on the surface (streaks) and a nanoscale depression attributed to locally enhanced resist exposure below a nanoparticle due to resonant excitation of a surface plasmon oscillation in the particle. (b) A cross-section through the imprint, showing a feature size of 50nm (~0.1λ).

not be excited exactly at their plasmon resonance frequency. However, a shift in the resonance frequency of ~1% as observed in the case of gold nanoparticles is small compared to the intrinsic linewidth of the plasmon resonance in the same Au nanoparticles, ensuring an even exposure even at such narrow spacing. Since the location of the plasmon resonance also depends on the shape of the nanoparticle,[15] one could ultimately consider correcting for nearest-neighbor induced resonance shifts by selectively altering the shape of individual nanoparticles in the mask.

It should be noted that the concave shape of the exposed area and the small thickness of the resist layer make pattern transfer via a lift-off process difficult. Another practical issue is the spacing between mask and substrate. Due to the short range of the field enhancement, the separation between mask and photoresist should be small (<10 nm). To allow for such small separation over large areas, conformable masks may be required. Even with these restrictions, we think this technique still has great potential for producing sub-diffraction-limit patterns in a parallel fashion using visible light and standard photoresist.

4. EXPERIMENTS

Our initial experiments were aimed at obtaining a proof-of-principle. To avoid difficulties in achieving the desired nanoscale spacing between mask and resist layer, instead of using a conventional mask our experiments involve 41 nm diameter silver nanoparticles (the "mask") spray-deposited onto a thin resist layer. Glass substrates (surface roughness < 5 Å RMS) were coated with standard g-line resist (AZ1813, Shipley), which has its maximum sensitivity in the wavelength range 300–450 nm. The resist was diluted with AZ EBR dilutant (ratio AZ1813:EBR = 1:4) and subsequently spin coated onto the substrates at 5000 rpm (60s) producing a smooth ~75 nm thick film. The smoothness is important since in the experiments ~40 nm diameter features need to be resolved. For illumination the output of a 1000 W Xe arc lamp was sent through a monochromator set to a wavelength of 410 nm, and subsequently passed through a polarizer to obtain polarization normal to the sample surface. The beam was vertically compressed using a cylindrical lens to increase the power density, and sent to the sample at glancing incidence. A photograph and a sketch of the illumination setup are shown in Fig. 5. The sample was suspended to prevent exposure by light scattered from the sample holder, see Fig. 5(b). The applied power densities were of the order of 1 mW/cm^2, and exposures times were in the range 10s – 300s. After exposure the films were developed for 20s in developer (MF317), mixed with water in a 1:1 ratio to slow down development. Conventional exposure of the 75 nm thick resist layers showed normal development at these development conditions. The developed films were investigated using contact mode Atomic Force Microscopy.

The developed films were found to still have some residual nanoparticles on the surface. Using the AFM tip it was possible to move the particles over the surface, producing streaks in the AFM images. In addition to the particles,

nanoscale dips were observed in the resist film, suggesting enhanced exposure in sub-wavelength size areas. Figure 6(a) shows an AFM scan of a 300×300 μm area, showing an approximately circular depression in the resist layer. Figure 6(b) shows a cross-section through the depression, showing a lateral size of approximately 50 nm, and a depth of 12 nm, possibly limited by the AFM tip shape. It should be noted that the identification of these nanoscale imprints is not fully unambiguous due to the relatively large resist roughness after development. Experiments are underway to further investigate the effect of plasmon enhanced resist exposure using e-beam defined masks containing a wide range of nanoparticle arrays.

CONCLUSIONS

We have shown that the local field enhancement occurring around metal nanoparticles when they are excited at the surface plasmon resonance frequency can be used to print nanoscale features in thin resist layers. Feature sizes below $\lambda/10$ can be generated in a parallel fashion using visible illumination and standard g-line photoresist.

ACKNOWLEDGEMENTS

REFERENCES

[1] M. Rothschild, T. M. Bloomstein, J. E. Curtin, D. K. Downs, T. H. Fedynyshyn, D. E. Hardy, R. R. Kunz, V. Liberman, J. H. C. Sedlacek, R. S. Uttaro, A. K. Bates, and C. Van Peski, J. Vac. Sci. Technol. B **17**, 3262 (1999)

[2] C. W. Gwyn, R. Stulen, D. Sweeney, and D. Attwood, J. Vac. Sci. Technol. B **16**, 3142 (1998)

[3] J. P. Silverman, J. Vac. Sci. Technol. B **16**, 3137 (1998)

[4] M. A. McCord, J. Vac. Sci. Technol. B **15**, 2125 (1997)

[5] J. Melngailis, Nucl. Instr. & Meth. B **80**, 1271 (1993)

[6] M.A. McCord and R. F. W. Pease, J. Vac. Sci. Technol. B **1**, 86 (1986)

[7] E. Betzig and J. K. Trautman, Science **257**, 189 (1992)

[8] X. M. Zhao, Y. N. Xia, and G. M. Whitesides, J. Mat. Chem. **7**, 1069 (1997)

[9] M. M. Alkaisi, R. J. Blaikie, S. J. McNab, R. Cheung, and D. R. S. Cumming, Appl. Phys. Lett. **75**, 3560 (1999)

[10] R. J. Blaikie, and S. McNab, Appl. Opt. **40**, 1692 (2001)

[11] S. J. McNab, and R. J. Blaikie, Appl. Opt. **39**, 20 (2000)

[12] P. G. Kik, S. A. Maier, and H. A. Atwater, Mat. Res. Soc. Symp. Proc. **705**, Y3.6 (2002)

[13] B. Lamprecht, A. Leitner, and F. R. Aussenegg, Appl. Phys. B **64**, 269 (1997)

[14] S. A. Maier, M. L. Brongersma, P. G. Kik, and H. A. Atwater, Phys. Rev. B **65**, 193408 (2002)

[15] see e.g. C. Bohren and D. Huffman, *Absorption and Scattering of Light by Small Particles*, Wiley, New York, 1983